J. Biophotonics **7**, No. 10, 818–824 (2014) / **DOI** 10.1002/jbio.201300042

Journal of BIOPHOTONICS

FULL ARTICLE

Narrow terahertz attenuation signatures in *Bacillus thuringiensis*

Weidong Zhang[*,1], *Elliott R. Brown*[*,1], *Leamon Viveros*[1], *Kellie P. Burris*[2], *and C. Neal Stewart, Jr.*[2]

[1] Terahertz Sensor Laboratory, Depts. of Physics and Electrical Engineering, Wright State University, Dayton, OH, USA, 45435
[2] Department of Plant Sciences, University of Tennessee, Knoxville, TN, USA, 37996

Received 12 March 2013, revised 9 June 2013, accepted 10 June 2013
Published online 4 July 2013

Key words: Terahertz, spectroscopy, *Bacillus thuringiensis*, spore, vegetative cells, surface mode

Terahertz absorption signatures from culture-cultivated *Bacillus thuringiensis* were measured with a THz photomixing spectrometer operating from 400 to 1200 GHz. We observe two distinct signatures centered at ~955 and 1015 GHz, and attribute them to the optically coupled particle vibrational resonance (surface phonon-polariton) of *Bacillus* spores. This demonstrates the potential of the THz attenuation signatures as "fingerprints" for label-free biomolecular detection.

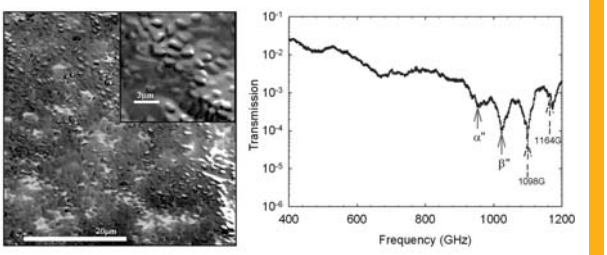

(left) The SEM photograph of Bt spores; (right) THz attenuation signatures attributed to surface phonon-polariton of Bt spores.

1. Introduction

It has been demonstrated that low terahertz (THz) vibrations of biomolecules can be detected by spectroscopic techniques, and the absorption signature profiles may be utilized for identification [1–4]. While a substantial number of reported works have focused on biomolecules such as DNA and RNA, there have been few studies in viruses, bacteria and whole cellular matrices. THz spectroscopy of bacteria is challenging because of the time-dependent biochemical processes and the multi-dimensional dynamic nature, but is of significance for potential applications in rapid label-free biological sensing. A notable effort in that direction is the observation of 250, 415 and 1035 GHz attenuation signatures in *Bacillus globigii* (Bg) [5].

In this paper we report the first-known THz measurements of *Bacillus thuringiensis* (Bt), a common soil bacteria and insect pathogen [6–8]. Upon sporulation, this bacteria produces bi-pyramidal protein crystals, δ-endotoxins or Cry proteins which are toxic to a variety of insects but are not harmful to humans. While Cry toxins have been widely applied as a "green" pestcide, recent use introduces Cry proteins into transgenic crops, providing a more targeted approach to insect management. The typical Bt cycle is shown in Figure 1, where the endospore and crystal are simultaneously present after an environmental stress induces sporulation, but then may be released after cell lysis. The spores can endure harsh environments such as aridity, extreme cold and heat and some radioactivity. When nutrition, temperature and other environmental conditions be-

* Corresponding authors: e-mail: weidong.zhang@wright.edu, e-mail: elliott.brown@wright.edu

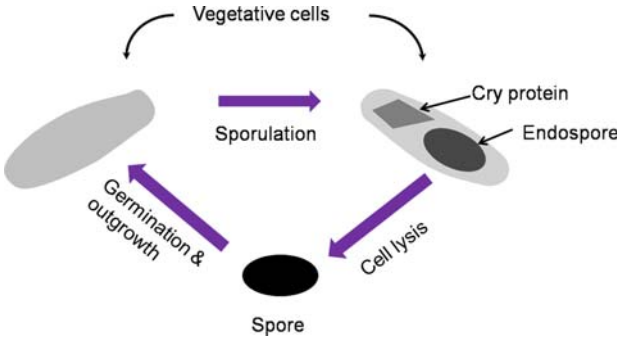

Figure 1 The cycle of *Bacillus* bacteria, [from sources, 9–10].

come favorable, spores germinate, develop into rapidly growing vegetative cells and begin another life cycle [9, 10].

More relevant to biosensing applications, Bt is in the same genus as *B. anthracis* and *B. cereus* of the *Bacillus* sp. [11]. The identification of THz signatures belonging to Bt could provide evidence for a new methodology of THz spectroscopic sensing for the security- and medically-relevant *B. anthracis* and *B. cereus*, but without the hazard. Indeed, as will be shown below, the THz absorption of *B. thuringiensis* displays repeatable, pronounced and unique fingerprint-type signatures.

2. Experiments

2.1 Samples

Bacillus thuringiensis subsp. kurstaki (Bt) strain was used for analysis. Four Bt samples labeled I–IV were tested. Starting from isolated stock bacteria, samples I and II were grown overnight in 50 ml tryptic soy broth (TSB; Becton, Dickinson, Sparks, MD) at 30 °C, 150 rpm. Bacterial cultures were transferred to a centrifuge tube, centrifuged at 5000 × g for 30 min, the liquid broth was removed, and then the bacteria were maintained at 4 °C for shipment. Samples I and II were collected 3 months apart. Samples III and IV were from the same isolated stock bacterial samples, but were grown on trypticase soy agar (TSA; TSB; Becton Dickinson, Sparks, MD; Agar: Fisher Scientific, Fair Lawn, NJ). Sample III was in log phase and sample IV was in late stationary phase.

The samples were cultured at the University of Tennessee, Knoxville, shipped overnight and were analyzed the following day. The samples were macroscopically examined upon receipt for purity and consistency prior to analysis.

2.2 Methods

The THz characterization was carried out with a state-of-the-art, high-resolution, frequency-domain photomixing spectrometer (Figure 2(a), (b)) [4], operated over the range 0.4 to 1.2 THz with a resolution (defined by the frequency step) of 500 MHz. This spectrometer has a high dynamic range, typically 70–80 dB at 100 GHz, and 40–50 dB at 1.0 THz.

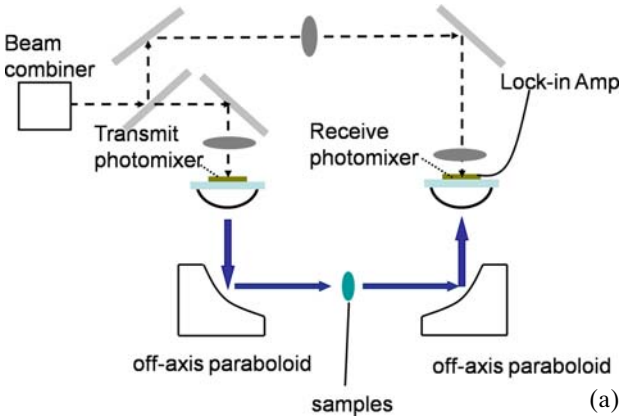

(a)

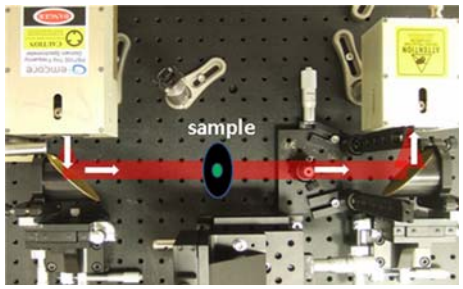

(b)

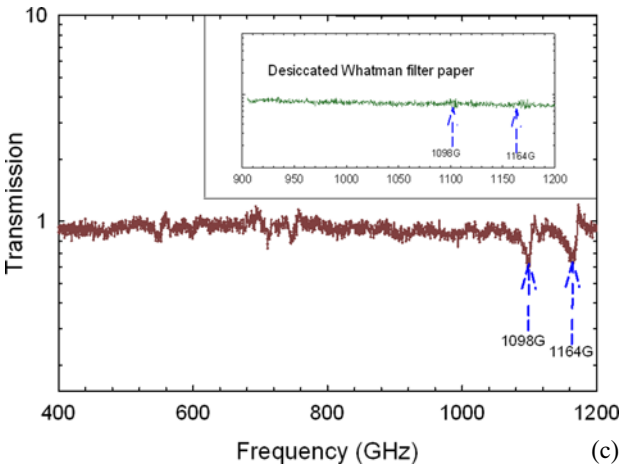

(c)

Figure 2 (**a**) The frequency-domain transmitter-receiver; (**b**) sample is placed in THz beam path (red line) for transmission; and (**c**) transmission results from Whatman filter paper. Inset: transmission of desiccated filter paper without water vapour lines.

The procedure of measurements was performed as follows. A Whatman #1 filter paper was placed in the THz beam path to obtain a background frequency scan recorded as P_B. A concentrated, ~0.2 mL sample of Bt bacteria (without broth or agar) was removed from a sealed plate or tube, and spread evenly over a 2 cm diameter with a spatula on the filter paper and immediately placed in the THz beam path with the signal recorded as P_S. The thickness of samples ranged from 200 to 600 μm. Then, the THz beam path was blocked completely for the frequency scan of the noise floor and recorded as P_N. The transmission was calculated from the sample signal, background, and noise floor as $T = (P_S - P_N)/(P_B - P_N)$.

To qualify our methodology, we first characterized the Whatman filter paper alone using the open-spectrometer scan as the background. In the resulting transmission of Figure 2(c), the Whatman paper was almost 100 percent transparent except where the two strong water-vapor lines occurred at 1098 and 1164 GHz, and the two weaker lines at 557 and 752 GHz. These lines were not present when the paper was desiccated and immediately characterized [inset of Figure 2(c)]. Therefore, the water lines were attributed to localized water vapor associated with residual liquid-state water in the filter-paper matrix.

3. Results and discussion

The transmission spectra of Bt samples I and II are plotted in Figure 3(a), (b), respectively.

As described above, four lines appear at 556, 752, 1098, and 1164, and another one at 987 GHz, all attributed to localized water vapor created by the Bt aqueous solution. Of greater interest are the other attenuation signatures: two from sample I at 917 GHz and 974 GHz [labelled α and β in Figure 3(a)], and two from sample II at 955 and 1015 GHz [labelled α' and β' in Figure 3(b)]. They are all significantly strong and independent of any water-vapor lines, so are attributed to the Bt samples. β is weaker than α because it's near the 987 GHz water vapor line.

To understand the origin of the Bt signatures, a second set of measurements was conducted with freshly harvested samples amenable to immediate inspection by high-powered microscopy. Sample III weighed 0.135 g and sample IV weighed 0.060 g and were evenly spread over the same area (~1.7 cm^2) for analysis. Excellent SNR ratios were obtained with both samples according to the background-sample-noise curves in Figure 4(a) and 5(a). In the THz transmission spectrum for sample III [Figure 4(b)], two signatures are evident that are very similar to α' and β' of sample II. However, they are both shifted slightly upward in center frequency, and therefore labelled α'' and β'' in Figure 4(b).

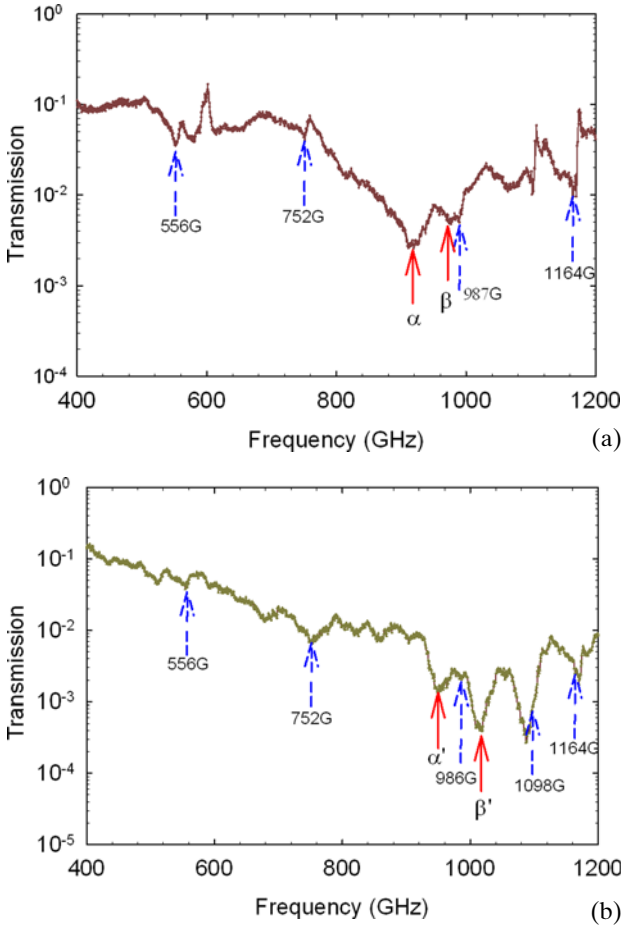

Figure 3 Transmission results from: (**a**) Bt samples I, and (**b**) II. The blue arrows denote the water-vapor lines.

In contrast, the transmission spectrum for sample IV [Figure 5(b)] shows no signatures in the 1.0 THz region. To check for any biological difference between samples III and IV, photographs were taken using a scanning electron microscope (SEM), as displayed in Figures 4(c) and 5(c), respectively. Clearly, sample III is replete with ellipsoid spores, seen most clearly in the magnified inset of Figure 4(c). The spores are approximately 1 μm in length and 0.4 μm in width, consistent with previous microscopic characterization [12]. In comparison, Figure 5(c) indicates that sample IV contains few if any spores. Instead, it is replete with rod-shaped vegetative cells of ~5 μm in length, also consistent with previous studies [13]. The likely reason for the difference between samples III and IV was the different stages of growth, III being in log phase and IV being in late stationary phase.

All the samples were freshly harvested during analysis, and they became visibly dried after about an hour changing from glossy to matte. The strong

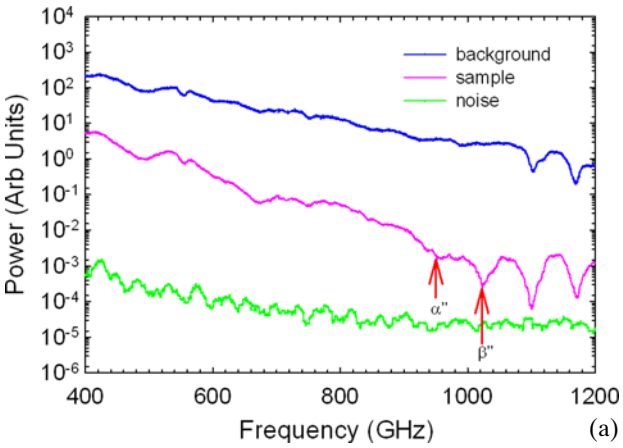

(a)

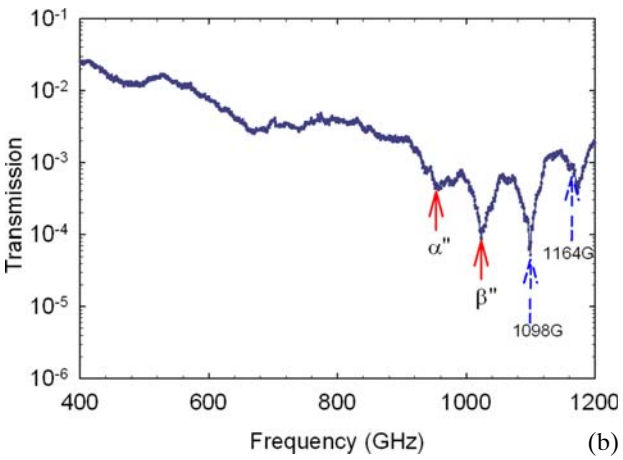

(b)

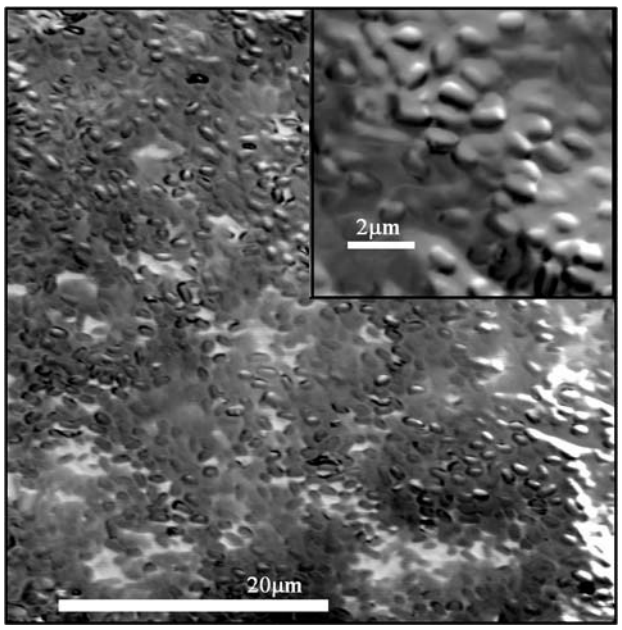

(c)

Figure 4 Bt sample III: (**a**) background, sample signal and noise floor; (**b**) transmission; and (**c**) SEM image (5000X).

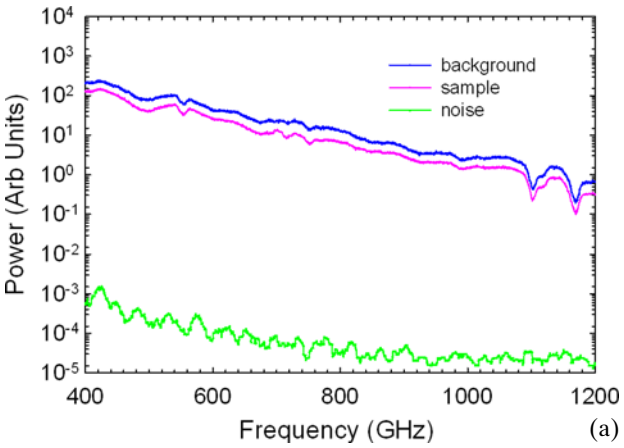

(a)

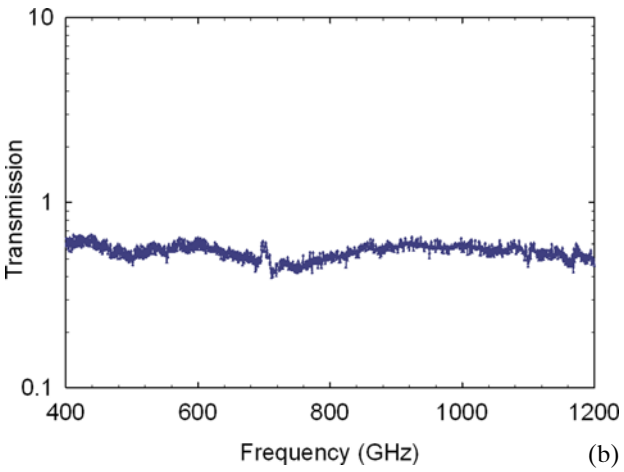

(b)

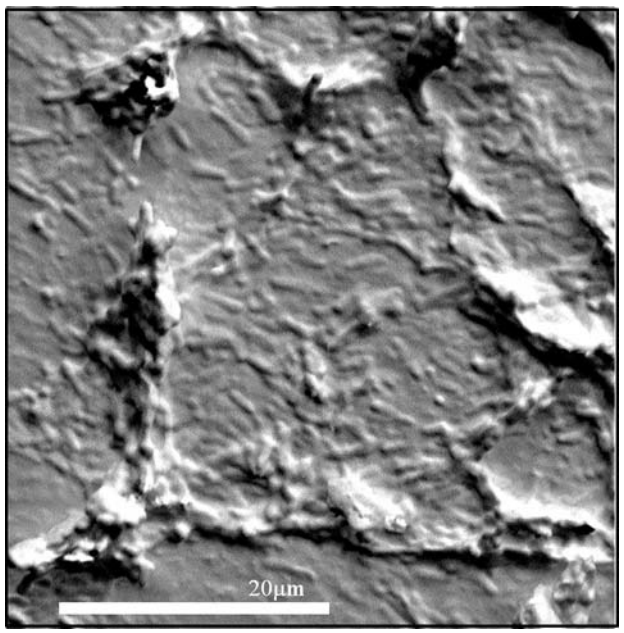

(c)

Figure 5 Bt sample IV: (**a**) background, sample signal and noise floor; (**b**) transmission; and (**c**) SEM image (5000X).

water attenuation across the range 400–1200 GHz weakens the multi-reflection effect. This applies to both the α and β absorptions: no periodic patterns were observed around either one.

The stark contrast between samples III and IV suggests that the two THz signatures from sample III, α'' and β'', are associated with the endospores. On first thought, this might seem unlikely since the spores are so much smaller than the THz wavelength ($\lambda \sim 300\,\mu m$) and have neither obvious mode of vibrational resonance nor the polarity necessary to absorb radiation even with a strong vibrational resonance. However, as will be analyzed physically below, and developed previously for *Bacillus subtilis* spores [5], the Bt spores can support a resonant *particle vibration* – the microscopic analog to the mechanical vibrations of macroscopic solid objects, such as tuning forks. Furthermore, in the aqueous environment, the spore outer coat becomes polarized by water dipoles. So if the vibrational resonance frequency of the spore greatly exceeds the Debye relaxation frequency of the water (~17 GHz at room temperature), the vibration can absorb radiation with high quality factor (narrow linewidth) and relatively low screening by the water dipoles.

4. Analysis of THz signatures

The outermost shell of Bt endospore – the exosporium – has a unique basal-layer structure according to recent electron microscopy and atom force microscopy alaysis [14]. The basal layer is in the form of a two dimentional (2D) crystal with the primitive unit cell composed of a biocomposite of proteins, lipids, and carbohydrates. For such a biomolecular crystal, THz frequency optical-phonon vibration can exist. This type vibration – adjacent different kinds of atoms moving in opposite directions within a unit cell – can couple with THz waves, resulting in polaritonic absorption as described by lattice dynamics theory [15]. This is the physical origin of particle vibrational resonance.

Phenomenologically, the frequency of optical phonon vibration on a spore surface is $\omega_t = 2\pi f_t$. The dielectric constant of spore surface is written as $\varepsilon(\omega) = \varepsilon_0 + \omega_p^2/(\omega_t^2 - \omega^2 - j\gamma\omega)$, where ε_0 is the background dielectric constant, γ is the damping constant and ω_p is the effective plasmon frequency. ω_p is calculated from $\omega_p = q\sqrt{\varrho_c/M}$ with q – the effective charge (thus the degree of polarity of the spore), M – the mass per primitive cell (of the spore's surface crystaliline structure) and ϱ_c – the density of the primitive cells (hence the density of optical phonons) [5, 16].

The THz field acts in the "quasistatic" limit, meaning that the instantaneous long-wavelength electric field is uniform across the much smaller spore. This allows application of the electromagnetic theory of small particles, which predicts a Lorentzian attenuation [16],

$$A_b \propto \gamma \frac{1}{[1 + L_i(\xi - 1)]^2} \frac{\omega_p^2}{[(\omega^2 - \omega_s^2)^2 + \omega^2\gamma^2]} \quad (1)$$

ω_s is the surface vibrational resonant frequency,

$$\omega_s^2 = \omega_t^2 + \frac{L_i\omega_p^2}{\varepsilon_m[1 + L_i(\xi - 1)]} \quad (2)$$

where L_i is unitless shape factor, ε_m is dielectric constant of surrounding environment, and ξ is a ratio between dielectric constants (spore/environment) [16].

Since the shape of a Bt spore is a spheroid, there are two shape factors: one is L_1 with degeneracy $d_\alpha = 1$ and the other is $L_2 = L_3$ with degeneracy $d_\beta = 2$. Eqation (2) predicts there are only two absorption lines, which are consistent with our experimental results.

According to Eq. (1), the resonance attenuations: α and β in Figure 3(a), α' and β' in Figure 3(b), α'' and β'' in Figure 4(b) are fit with the Lorentzian line shape, $\log(T) \propto [A_b(\omega) + B]$, where B is background attenuation mostly from water moisture and T is the transmission. Then the surface vibrational resonant frequencies ω_s are extracted.

The fitting results for α, α' and α'' are plotted in Figure 6. α is centered at 917 GHz, α' is centered at 955 GHz and α'' is centered at 966 GHz. The damping constants are $\gamma = 84$ GHz, $\gamma = 66$ GHz and $\gamma = 135$ GHz, respectively. The fitting results for β,

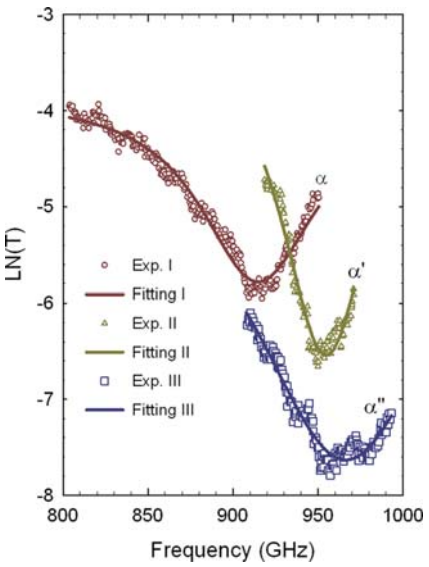

Figure 6 The Lorentzian fittings of α, α' and α''.

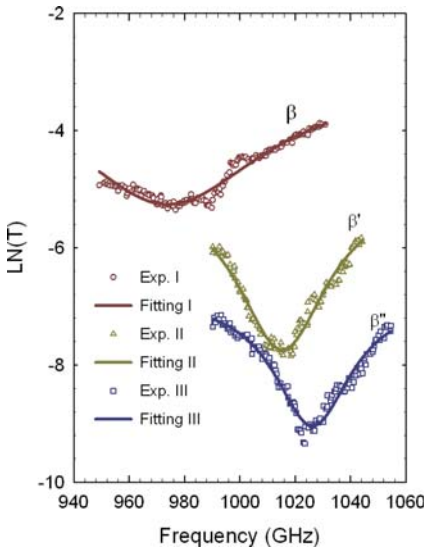

Figure 7 The Lorentzian fittings of β, β' and β''.

β' and β'' are plotted in Figure 7. β is centered at 974 GHz, β' is centered at 1015 GHz and β'' is centered at 1026 GHz. The damping constants are $\gamma = 85$ GHz, $\gamma = 40$ GHz and $\gamma = 34$ GHz, respectively.

As shown Table 1, β'' is shifted 11 GHz relative to β'; β' is shifted 41 GHz relative to β, but β'', β' and β are the same signature. The shift between α'' between α' is 11 GHz; the shift between α' and α in Figure 3(a) is ~38 GHz, but again, α'', α' and α are the same signature.

The results reported here and our other experiments support that the differences of α, α' and α'' (along with β, β' and β'') were related to the hydration level of spore samples. For a less hydrated sample, the frequency of the major signature (α) was higher, typically around 955 GHz. For a fresh (normal hydration) sample harvested directly from an agar plate, the frequency of α was 917 GHz. When a sample was completely dry, neither signature appear in its spectrum.

In a separate experiment, two consecutive measurements of the same Bt sample 44 minutes apart were recorded. We observed that the α signature near the 917 GHz increased about 38 GHz, the same as reported above. The unsealed sample remained stationary in the THz path without any disturbance.

Table 1 The resonance frequencies of α, α', α'', β, β', and β''.

	α (GHz)	β(GHz)
sample I	917	974
sample II	955	1015
sample III	966	1026

The attenuation across the whole range of 400–1200 GHz roughly reduced by ~18 dB suggesting the loss of moisture as the sample was exposed to air since liquid water is highly absorbing in the THz regime. This demonstrated the link between THz signatures and the hydration level of the Bt sample. The movement of THz signatures accompanying the hydration further supports that the source of absorption is likely from the outer protein layer of spores which is the first part of the spore that is subject to dehydration and alters quickly due to the environmental change.

Other possible factors causing the shift of the resonant frequency, according to Eq. (2), include the variation of spore's dielectric environment (ε_m) as well as the shape factor (L_i). But, overall, the 917 GHz and 955 GHz were the two frequencies we kept seeing in the tested Bt spore samples.

5. Conclusion

In summary, we report the distinctive THz bands of Bt bacterial spores. The attenuation signatures were attributed to the optically coupled particle vibrational resonance – surface phonon polarition- – of Bt spores, and a pronounced signature was measured at ~917 or ~955 GHz depending on the hydration of spore samples. These signatures were reproducible, but they were not present in Bt vegetative cells without spores. Studies are underway to explore species discrimination. The discriminatory data will be addressed in an upcoming publication. Hence our research demonstrates a practical, label-free THz spectroscopic sensing method of bacterial spores.

Acknowledgements This material is based upon work supported by, or in part by, the U.S. Army Research Laboratory and the U.S. Army Research Office under contract number W911NF-11-1-0024.

Author biographies Please see Supporting Information online.

References

[1] E. R. Brown, J. E. Bjarnason, A. M. Fedor, and T. M. Korter, Applied Physics Letters **90**, 061908 (2007).
[2] T. R. Globus, D. L. Woolard, T. Khromova, T. W. Crowe, M. Bykhovskaia, B. L. Gelmont, J. Hesler, and A. C. Samuels, Journal of biological physics **29**, 89 (2003).
[3] B. M. Fischer, M. Franz, and D. Abbott, IRMMW06, **wedB6-2**, 362 (2006).

[4] E. R. Brown, E. A. Mendoza, Y. Kuznetsova, A. Neumann, and S. R. J. Brueck, in: Terahertz and Mid Infrared Radiation: Generation, Detection and Applications, (NATO Science for Peace and Security Series B: Physics and Biophysics, ed. by M. F. Pereira and O. Shulika (Springer, New York, 2011), chap. 3, pp. 15–22.
[5] E. R. Brown, T. B. Khromova, T. Globus, D. L. Woolard, J. O. Jensen, and A. Majewski, IEEE Sensors Journal **6**, 1076 (2006).
[6] A. Bravo, S. S. Gill, and M. Soberón, Toxicon **49**, 423 (2007).
[7] N. Galitsky, V. Cody, A. Wojtczak, D. Ghosh, J. R. Luft, W. Panghorn, and L. English, Acta Crystallographica Section D **57**, 1101 (2001).
[8] J. Li, J. Carroll, and D. J. Ellar, Nature **353**, 815 (1991).
[9] M. J. L. De Hoon, P. Eichenberger, and D. Vitkup, Current Biology **20**, 0960 (2010).
[10] V. Sanchis, http://www.komunich.de/vincent-sanchis/france/bacillus-thuringiensis.html.
[11] D. Xu and J.-C. Côté, Applied and Environmental Microbiology **72**, 4653 (2006).
[12] M. Plomp, T. J. Leighton, K. E. Wheeler, and A. J. Malkin, Langmuir **21**, 7892–7898 (2005).
[13] H. Sakai, M. T. Howlader, Y. Ishida, A. Nakaguchi, K. Oka, K. Ohbayashi, M. Yamagiwa, and T. Hayakawa, Journal Of Bioscience and Bioengineering **103**, 381 (2007).
[14] L. Kailas, C. Terry, N. Abbott, R. Taylor, N. Mullin, S. B. Tzokov, S. J. Todd, B. A. Wallace, J. K. Hobbs, A. Moir, and P. A. Bullough, in: Proceedings of the National Academy of Sciences, Vol. 108 (2011), p. 16014.
[15] M. Born and K. Huang, Dynamical Theory of Crystal Lattices (Oxford University Press, 1998).
[16] C. F. Bohren and D. R. Huffman, Absorption and Scattering of Light by Small Particles (Wiley, New York, 1983), chap. 9 and 12.

